scientific reports

Check for updates

OPEN

Genome-wide association study of subfoveal choroidal thickness in a longitudinal cohort of older adults

Hyeong Min Kim[1,6], Kwangsic Joo[1], Minji Kim[1], Young Joo Park[1], Ji Won Han[2], Ki Woong Kim[2,3,4], Sejoon Lee[5] & Se Joon Woo[1]✉

To identify genetic influences on subfoveal choroidal thickness of older adults using a genome-wide association study (GWAS). We recruited 300 participants from the population-based Korean Longitudinal Study on Health and Aging (KLoSHA) and Korean Longitudinal Study on Cognitive Aging and Dementia (KLOSCAD) cohort studies and 500 participants from the Bundang age-related macular degeneration (AMD) cohort study dataset. We conducted a GWAS on older adult populations in the KLoSHA and KLOSCAD cohorts. Single nucleotide polymorphisms (SNPs) associated with choroidal thickness were identified with *P* values $< 1.0 \times 10^{-4}$ in both the right and left eyes, followed by validation using the Bundang AMD cohort dataset. This association was further confirmed by a functional in vitro study using human umbilical vein endothelial cells (HUVECs). The ages of the cohort participants in the discovery and validation datasets were 73.5 ± 3.3 and 71.3 ± 7.9 years, respectively. In the discovery dataset, three SNPs (rs1916762, rs7587019, and rs13320098) were significantly associated with choroidal thickness in both eyes. This association was confirmed for rs1916762 (genotypes GG, GA, and AA) and rs7587019 (genotypes GG, GA, and AA), but not for rs13320098. The mean choroidal thickness decreased by 56.7 µm (AA, 73.8%) and 31.1 µm (GA, 85.6%) compared with that of the GG genotype of rs1916762, and by 55.4 µm (AA, 74.2%) and 28.2 µm (GA, 86.7%) compared with that of the GG genotype of rs7587019. The SNPs rs1916762 and rs7587019 were located close to the *FAM124B* gene near its cis-regulatory region. Moreover, *FAM124B* was highly expressed in vascular endothelial cells. In vitro HUVEC experiments showed that the inhibition of *FAM124B* was associated with decreased vascular endothelial proliferation, suggesting a potential mechanism of choroidal thinning. *FAM124B* was identified as a susceptibility gene affecting subfoveal choroidal thickness in older adults. This gene may be involved in mechanisms underlying retinal diseases associated with altered choroidal thickness, such as age-related macular degeneration.

Keywords Age-related macular degeneration (AMD), Single nucleotide polymorphism (SNP), Choroidal thickness, GWAS, CUL3, FAM124B, HUVEC

Choroidal vascular structure and its alterations are associated with various retinal diseases, such as age-related macular degeneration (AMD), polypoidal choroidal vasculopathy (PCV), and central serous chorioretinopathy (CSC)[1–4]. The development of the enhanced depth imaging (EDI) technique of spectral-domain optical coherence tomography (SD-OCT) has enabled clinicians to discern details of choroidal structure and accurately measure its thickness[5,6]. Using the SD-OCT EDI mode, a subfoveal choroidal thickness (SFCT) analysis demonstrated that PCV presented with thickening of the choroid, whereas exudative AMD showed choroidal thinning[7]. Similarly, as clinicians continue to focus on the choroidal layer in retinal diseases, the term "pachychoroid" has been introduced to describe a spectrum of diseases characterized by clinically significant choroidal thickening with dilated large choroidal vessels and overlying choriocapillaris[8].

[1]Department of Ophthalmology, Seoul National University College of Medicine, Seoul National University Bundang Hospital, 173-82 Gumi-ro, Bundang-gu, Seongnam-si 13620, Gyeonggi-do, Republic of Korea. [2]Department of Neuropsychiatry, Seoul National University Bundang Hospital, Seongnam, Republic of Korea. [3]Department of Psychiatry and Behavioral Science, Seoul National University College of Medicine, Seoul, Republic of Korea. [4]Department of Brain and Cognitive Science, Seoul National University College of Natural Sciences, Seoul, Republic of Korea. [5]Precision Medicine Center, Seoul National University Bundang Hospital, Seongnam, Republic of Korea. [6]Department of Ophthalmology, Konkuk University School of Medicine, Seoul, Republic of Korea. ✉email: sejoon1@snu.ac.kr

Recent genome-wide association studies (GWAS) have identified susceptibility genes for AMD, PCV, and CSC. Notably, single nucleotide polymorphism (SNP) rs1061170 in the complement factor H (*CFH*) gene located on chromosome 1q31 was reported in 2005[9–11]. Subsequently, numerous SNPs and genes, including *ABCA1*, *APOE*, *ARMS2/HTRA1*, *B3FALTL*, *CFI*, *C2*, *C3*, *COL4A3*, *GATA5*, *LIPC*, *MMP9*, *TIMP3*, *TNFRSF10A*, and *VIPR2*, were discovered using GWAS[12–19]. Furthermore, efforts to correlate susceptibility genes (genotypes) and clinical phenotypes have been increasing. Mori et al. reported a shared genetic susceptibility between PCV and macular neovascularization secondary to CSC[17]. Mori noted that the *ARMS2*, *CFH*, *COL4A3*, and *B3GALTL* genes have been recognized as susceptibility genes for CSC development and mentioned that these four genes are also associated with AMD susceptibility. Thee et al. from the EYE-RISK consortium analyzed AMD features and macular thickness following the harmonization of genetic data[19]. Their findings suggested that risk variants at *ARMS2/HTRA1* exhibit an increased risk of late AMD progression, with phenotypes resembling the complement pathway variants. Since retinal and choroidal morphological changes are linked to disease patterns and visual outcomes, exploring the potential association between genetic discoveries and structural phenotypes is crucial. Changes in choroidal thickness are a critical feature of retinal diseases, including AMD, and are likely to be involved in their pathogenesis. However, no GWAS has targeted choroidal thickness.

Therefore, in this study, we investigated genetic influences affecting the SFCT using a GWAS in an older adult population-based cohort, identified susceptibility genes affecting choroidal structure, and validated the association using an AMD cohort. Our previous study using the KLoSHA-Eye study cohort revealed that SNPs in *CFH gene* (Y402H, rs1061170) is a genetic risk factor associated with choroidal thinning in eyes of the normal elderly population[23]. In this subsequent study, our goal is to identify the genes influencing the choroidal thickness within the population cohort using GWAS and compare these findings with the previous Bundang AMD cohort to uncover potentially relevant SNPs that could impact the choroid and contribute to the development of AMD. Additionally, we conducted a functional experiment using human umbilical vein endothelial cells (HUVECs) to investigate the in vitro effects of the altered expression of associated genes.

Materials and methods

The Institutional Review Board (IRB) of the Seoul National University Bundang Hospital (SNUBH) approved this study, which adhered to the principles of the Declaration of Helsinki (IRB No. B-1812/510-107). Written informed consent was obtained from all the participants.

Discovery dataset

We used the data of two population-based longitudinal cohort studies, which enrolled Korean elderly adults aged more than 60 years: the Korean Longitudinal Study on Health and Aging (KLoSHA) and Korean Longitudinal Study on Cognitive Aging and Dementia (KLOSCAD)[21,22]. All participants underwent comprehensive baseline ophthalmic examinations, including best-corrected visual acuity, intraocular pressure, auto kerato-refractometry, optical biometry with axial length calculation (IOL Master; Carl-Zeiss Meditec, Dublin, CA, USA), and spectral domain optical coherence tomography (SD-OCT; Heidelberg Engineering, Heidelberg, Germany). Two independent retinal specialists (H.M.K. and Y.J.P.) manually measured the SFCT using the EDI mode each time, and the average SFCT was analyzed. The SFCT was measured as the vertical perpendicular distance from the innermost hyperreflective line of the choroid-scleral interface to the hyperreflective line of Bruch's membrane. The left and right eyes were analyzed separately. Out of 454 individuals in the 2nd KLoSHA enrollment, 250 (55%) received eye examinations, including OCT. In the Yongin County KLosCAD enrollment, 250 out of 660 patients (38%) also completed these eye examinations, including OCT, resulting in a combined total of 500 patients. According to our previous study, 70 patients with ocular pathologies were excluded from the 500 participants who underwent the evaluations, resulting in a final count of 430 participants[22]. 75 patients with cognitive disorders and 55 patients unable to measure SFCT accurately were also excluded. Finally, a total of 300 participants were included in this study (Fig. 1). We excluded patients with significant myopia or hyperopia (axial length exceeding 26 mm or less than 22 mm), high intraocular pressure (greater than 21 mmHg), self-reported glaucoma history, and combined ocular pathologies, including age-related macular degeneration, epiretinal membrane, diabetic macular edema, and diabetic retinopathy found on OCT infrared imaging, which may affect subfoveal choroidal thickness.

Validation dataset

For the validation dataset, we used the Bundang AMD cohort[20,23]. This cohort included Korean adults aged more than 50 years who were initially diagnosed with non-exudative or exudative AMD in Seoul National University Bundang Hospital (SNUBH). A total of 500 participants were enrolled, and detailed ophthalmic assessments were performed, including color fundus photography and SD-OCT (Heidelberg Engineering, Heidelberg, Germany). Similar to the study dataset, two independent retinal specialists (H.M.K. and Y.J.P.) manually measured the subfoveal choroidal thickness each time, and the average SFCT was analyzed. Similarly, we excluded patients with significant myopia, high intraocular pressure, self-reported glaucoma history, and combined ocular pathologies other than AMD. In the validation dataset, only the right eye was used for the analysis.

GWAS analysis

GWAS genotyping was performed using the Illumina Human OmniExpress or Human Hap610-Quad bead chips. For replication, genotyping was performed using the MassArray platform (Sequenom) and TaqMan allelic discrimination probes (Applied Biosystems). A GWAS was conducted on choroidal thickness data from 300 participants (left and right eyes). For the left eye, 300 participants were analyzed after excluding 23 patients without data on choroidal thickness. For the right eye, 300 participants were analyzed, excluding 28 patients without data on choroidal thickness. The analysis was performed using the PLINK software, selecting variants

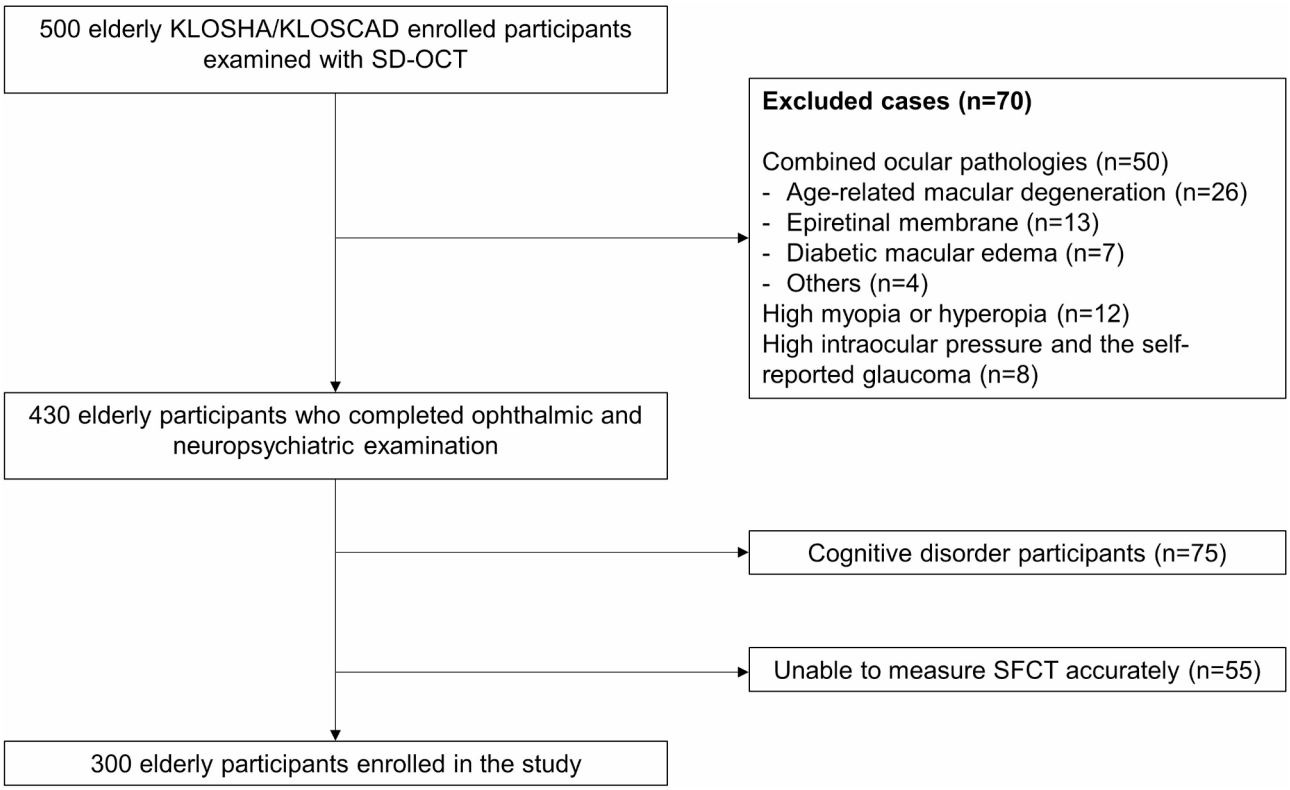

Fig. 1. A flow diagram of enrolled participants in this study.

based on genotyping mutations in more than 95% of samples, Hardy-Weinberg equilibrium (pHWE $\geq 10^{-6}$), and mutations present in more than 1% of all samples. An association study analyzed the choroidal thickness of the right and left eyes. Among the 590,000 SNPs examined, those with $P < 10^{-4}$ in both the left and right eyes were extracted.

In silico analysis using open data source

The captured Hi-C data in the GM12878 cell line were visualized using the 3D Genome Browser from the YUE Laboratory (http://3dgenome.fsm.northwestern.edu/view.php). GTEx (https://gtexportal.org/home/) was used to identify interacting genes regulated by candidate SNPs and to analyze target gene expression using bulk RNA sequencing data across multiple tissues. The Protein Atlas (https://www.proteinatlas.org/) and Expression Atlas (https://www.ebi.ac.uk/gxa/home) were used to analyze cell type-specific RNA and gene expression data at the single-cell level. Single-cell-specific patterns were visualized by modifying the Tabula Sapiens data (https://tabula-sapiens-portal.ds.czbiohub.org/).

HUVEC experiment

Cell culture

HUVECs (cat no. 4453, Sartorius, Germany) were purchased from Sartorius and used in the study. The cells were cultured in a cell incubator at a temperature of 37 °C and with 5% CO_2. Endothelial Cell Growth Medium 2 (EGM-2, cat no. C-22011, PromoCell, Germany) supplemented with 1% penicillin/streptomycin (cat no. L0018, BioWest, France) was used as the culture medium. The medium was replaced every 48 h, and the cells were passaged upon reaching 70–80% confluence. Cells passaged between two and five times were used in the experiments.

Small interfering ribonucleic acid (siRNA) Transfection

FAM124B (Human) 3 unique 27-mer siRNA duplexes (cat no. SR312644, OriGene, USA) were purchased from OriGene and used in the study. The sequences of the siRNAs were as follows: 5'-AUGUUCUAGAAAUGGA GUACUGACC-3', 5'-GCAGUUUAAGGUUCAAGAGAUCGGC-3', and 5'-GGCUUGACCAUCAUAAAUUC UGAAC-3'. For transfection, Lipofectamine 3000 (cat no. L3000001, Invitrogen, USA) was purchased and the experiments were conducted according to the manufacturer's instructions. Approximately $3–4 \times 10^4$ cells were seeded per well in an 8-well Lab-Tek II Chamber Slides (cat no. 154534, Thermo Scientific, USA). When the cells reached 70–90% confluence under conditions of 37 °C and 5% CO_2, Lipofectamine 3000 reagent (0.15 and 0.3 µL) and Opti-MEM medium (cat no. 31985070, Gibco, USA) were mixed according to the manufacturer's instructions, along with 0.2 µg siRNA, 0.4 µL P3000 reagent, and 10 µL Opti-MEM medium in a 1:1 ratio. The mixture was then incubated at room temperature for 15 min. The resulting mixture was added to each well and

incubated at 37 °C and 5% CO_2 for 48 h. Immunofluorescence was performed 48 h after siRNA treatment, with the timing of the siRNA treatment as the reference point.

Immunofluorescence
The siRNA-treated HUVECs were fixed with a 4% paraformaldehyde solution at room temperature for 5 min and subsequently with 100% methanol at -20 °C for 5 min. After two washes with phosphate-buffered saline (PBS), the fixed cells were blocked using a blocking buffer (5% fetal bovine serum (FBS), 5% goat serum, 0.1% Triton-X 100, 0.02% sodium azide in PBS) at room temperature for 10 min. To detect FAM124B protein, an anti-FAM124B antibody (cat no. 21313-1-AP, Proteintech, Germany) was used, followed by Alexa Fluor 488 goat anti-rabbit IgG secondary antibody (cat no. A-11008, Invitrogen, USA). To detect Ki67, an anti-Ki67 antibody (cat no. STJ119231, St John's Laboratory, UK) was used, followed by Alexa Fluor 594 goat anti-rabbit IgG secondary antibody (cat no. A-11012, Invitrogen, USA). The samples were observed under a fluorescence microscope (Axio imager M2, Carl Zeiss, Germany).

Cell migration and invasion assay
One million (1×10^6) HUVECs were seeded into each well of a six-well tissue culture plate containing 2 ml of M199 medium supplemented with 20% FBS and antibiotics. The cells were left to grow overnight to achieve nearly full coverage of the well. To inhibit cell proliferation, 5 µg/mL of mitomycin C (100 µL from a stock of 100 µg/mL) was added to the medium 2 h before creating a scratch. An aseptic P-200 pipette tip was used to create a controlled scratch wound by drawing a line across the center of each well to simulate an artificial wound in the cell layer. Both the control and FAM124B siRNA knockdown transfections were performed immediately after the scratch was created. The plate was subsequently placed in a CO_2 incubator for a 24-h period after transfection. The cells were then rinsed with PBS, stained using a 0.5% crystal violet solution, observed, photographed, and quantified using an inverted microscope. The migrated area was calculated by subtracting the area without cells at each time point from the area without cells at 0 h, and then dividing this area by the area without cells at 0 h.

Results

In total, 300 and 500 participants met the inclusion criteria for the KLoSHA/KLOSCAD discovery and Bundang AMD validation cohorts, respectively. The participants' ages at the first visit in the cohort dataset were 73.5 ± 3.3 years and 71.3 ± 7.9 years, respectively. The sex ratios (male: female) were 153:147 (51%:49%) and 296:204 (59%:41%), respectively. The GWAS analysis revealed three SNPs were associated with subfoveal choroidal thickness: rs1916762 at chromosome 2 (intergenic, 24 kb from *FAM124B* and 44 kb from *CUL3*, left eye $P=6.55\times10^{-5}$, right eye $P=9.13\times10^{-6}$); rs7587019 at chromosome 2 (intergenic, 37 kb from FAM124B and 30 kb from *CUL3*, left eye $P=3.80\times10^{-5}$, right eye $P=6.65\times10^{-5}$); and rs13320098 at chromosome 3 (intergenic, 81 kb from *MIR466* and 288 kb from *STT3B*, left eye $P=2.24\times10^{-5}$, right eye $P=8.68\times10^{-6}$) (Table 1 and Fig. 2).

The discovery and validation cohort datasets were classified into three genotypes: reference/reference alleles, reference/alternative alleles, and alternative/alternative alleles (Tables 1 and 2). The average age and sex proportions did not differ significantly among the three genotypes in each cohort dataset (Table 2). The SFCT was significantly different between the rs1916752 and rs7587019 genotypes in both the discovery and validation datasets ($P<0.001$). Meanwhile, the SFCT in the rs13320098 SNP was significantly different among the genotypes in the discovery cohort ($P<0.001$), but not in the validation cohort ($P=0.149$) (Table 2). No significant difference in the SFCT was observed between the left and right eyes within each genotype in the study cohort. Figure 3 summarizes the association between the SFCT and the genotypes of the three SNPs. Post-hoc analyses revealed that choroidal thickness significantly differed between the rs1916762 and rs7587019 genotypes. However, there was no significant difference in choroidal thickness between the TT and TC genotypes of rs13320098 in the validation cohort (Fig. 3): rs1916762 GG 226.0 ± 35.0 µm (100.0%), GA 173.0 ± 31.5 µm (76.5%), and AA 147.4 ± 33.3 µm (65.2%); rs7587019 GG 226.6 ± 36.0 µm (100.0%), GA 172.4 ± 31.3 µm (76.1%), and AA 149.5 ± 34.6 µm (65.9%); and rs13320098 TT 169.1 ± 41.6 µm (100.0%), TC 171.1 ± 38.4 µm (101.1%), and CC 149.2 ± 43.2 µm (88.2%) (Table 2).

Because the two SNPs were non-coding variants, we investigated their chromosomal locations and utilized capture Hi-C data from the female B-cell lymphoblastoid cell line (GM12878) to identify specific genes regulated by these two SNPs. The rs1916762 and rs7587019 SNPs are located upstream of *FAM124B* and downstream of *CUL3* (Fig. 4A). Both SNPs were positioned close to *FAM124B*, near its cis-regulatory region. The captured

Chromosome	2	2	3
SNP	rs1916762	rs7587019	rs13320098
Base pair	225,290,792	225,304,551	31,285,081
Reference Allele	G	G	T
Alternative Allele	A	A	C
P-value (Left eye)	6.55×10^{-5}	3.80×10^{-5}	2.24×10^{-5}
P-value (Right eye)	9.13×10^{-6}	6.65E x 10^{-5}	8.68×10^{-6}
Gene (Intergenic)	24 kb from *FAM124B* / 44 kb from *CUL3*	37 kb from *FAM124B* / 30 kb from *CUL3*	81 kb from *MIR466* / 288 kb from *STT3B*

Table 1. GWAS results of SNPs with the greatest evidence of association for the subfoveal choroidal thickness.

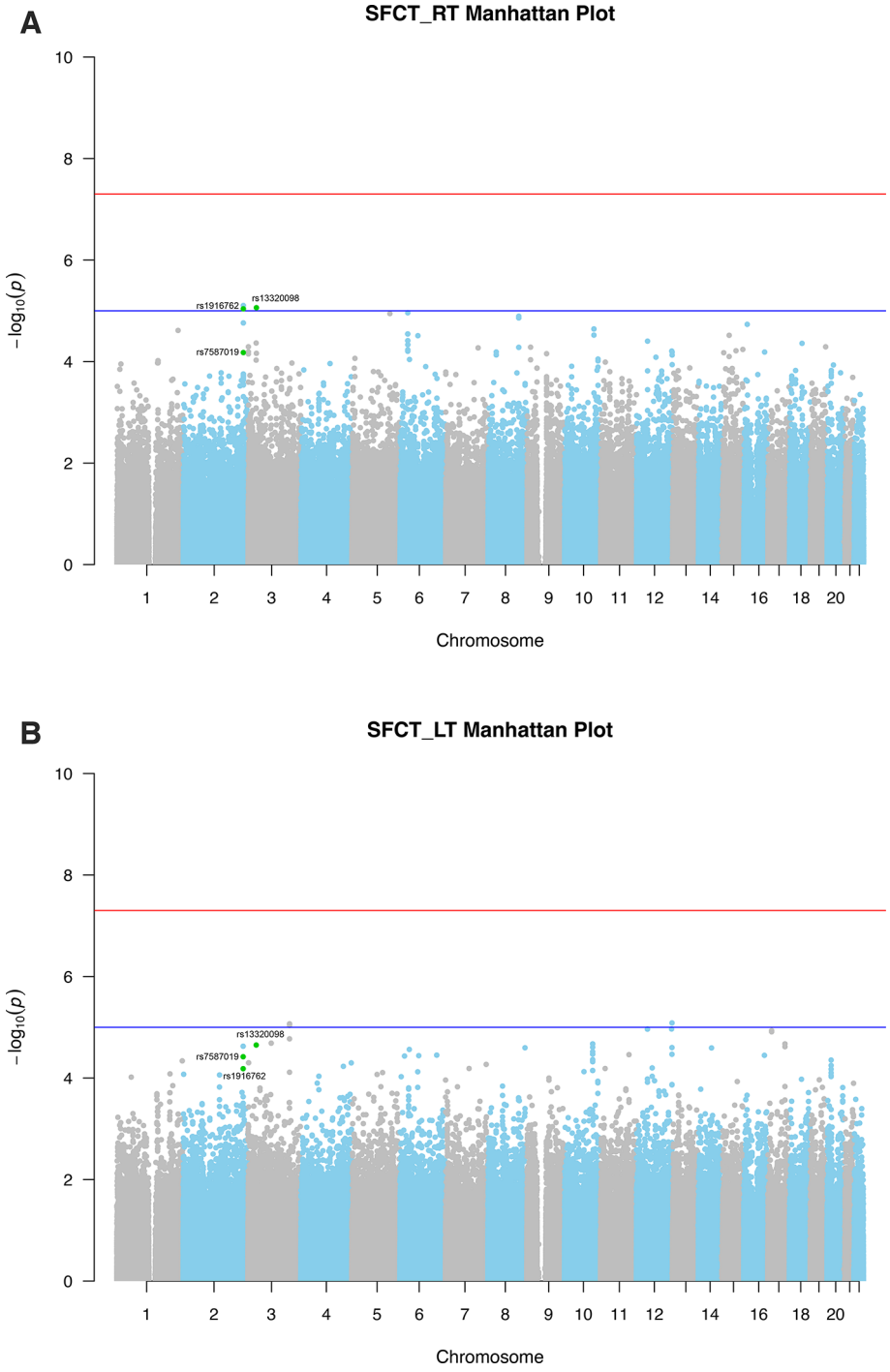

Fig. 2. Manhattan plots of subfoveal choroidal thickness (SFCT) measurements in the right eye (**A**), and the left eye (**B**).

Hi-C data revealed interactions between rs7587019 and the starting exons, including the promoter regions, of *FAM124B* and *CUL3*, suggesting that rs7587019 may play a role in regulating *FAM124B* and/or *CUL3* expression. Moreover, single-tissue expression quantitative trait loci (eQTLs) for the two GTEx variants predicted interactions with *FAM124B* across multiple tissues. Additionally, these two variants were predicted to interact with a long non-coding RNA (pseudogene) located in and near the *CUL3* gene (Table 3). Subsequently, we analyzed gene expression data, including bulk RNA sequencing, from the Protein Atlas to determine which gene among *FAM124B* and *CUL3* is regulated by the two SNPs. While *FAM124B* is expressed in many tissues such as the breast, colon, heart muscle, and arteries, it is notably enriched in endothelial cells (Fig. 4B, C). Conversely, *CUL3* is ubiquitously expressed in the cell nucleus and is particularly enriched in spermatids. Single-cell RNA sequencing from the Protein Atlas and Expression Atlas revealed that *FAM124B* is highly expressed in adipocytes

SNP / Gene	rs1916762 / FAM124B; CUL3							
Cohort	KLOSHA/KLOSCAD study				AMD validation			
Genotype	GG	GA	AA	*P*-value	GG	GA	AA	*P*-value
Number	122	136	42		208	229	63	
Age (years)	73.3 ± 3.4	73.8 ± 3.1	73.0 ± 3.4	0.312	71.3 ± 7.8	71.5 ± 8.6	70.8 ± 7.9	0.810
Sex (M: F)	65 : 57	68 : 68	20 : 22	0.791	130 : 78	131 : 98	35 : 28	0.436
Subfoveal (μm) choroidal thickness								
Left eye	220.7 ± 74.3	184.1 ± 66.9	162.6 ± 68.1	**< 0.001**	226.0 ± 35.0	173.0 ± 31.5	147.4 ± 33.3	**< 0.001**
Right eye	215.6 ± 62.2	184.3 ± 66.1	158.0 ± 58.7	**< 0.001**				
SNP / Gene	rs7587019 / FAM124B; CUL3							
Cohort	KLOSHA/KLOSCAD study				AMD validation			
Genotype	GG	GA	AA	*P*-value	GG	GA	AA	*P*-value
Number	130	131	39		216	224	60	
Age (years)	73.5 ± 3.6	73.5 ± 3.4	73.4 ± 3.0	0.972	71.2 ± 8.1	71.6 ± 8.4	70.7 ± 7.8	0.693
Sex (M: F)	65 : 65	63 : 68	19 : 20	0.956	134 : 82	130 : 94	32 : 28	0.427
Subfoveal (μm) choroidal thickness								
Left eye	217.5 ± 66.4	188.3 ± 65.6	158.6 ± 63.0	**< 0.001**	226.6 ± 36.0	172.4 ± 31.3	149.5 ± 34.6	**< 0.001**
Right eye	212.2 ± 59.1	185.0 ± 65.1	160.3 ± 60.1	**< 0.001**				
SNP / Gene	rs13320098 / MIR466;STT3B							
Cohort	KLOSHA/KLOSCAD study				AMD validation			
Genotype	TT	TC	CC	*P*-value	TT	TC	CC	*P*-value
Number	216	78	6		361	124	15	
Age (years)	73.7 ± 3.4	73.3 ± 3.5	71.5 ± 4.2	0.219	71.2 ± 8.2	71.3 ± 8.3	74.6 ± 5.9	0.310
Sex (M: F)	99 : 117	41 : 37	3 : 3	0.208	207 : 154	82 : 42	7 : 8	0.138
Subfoveal (μm) choroidal thickness								
Left eye	191.8 ± 73.4	162.1 ± 68.8	115.9 ± 25.1	**< 0.001**	169.1 ± 41.6	171.1 ± 38.4	149.2 ± 43.2	0.149
Right eye	188.9 ± 71.0	161.8 ± 62.9	94.9 ± 44.5	**< 0.001**				

Table 2. Demographics and clinical characteristics of KLOSHA/KLOSCAD study cohort and AMD validation cohort.

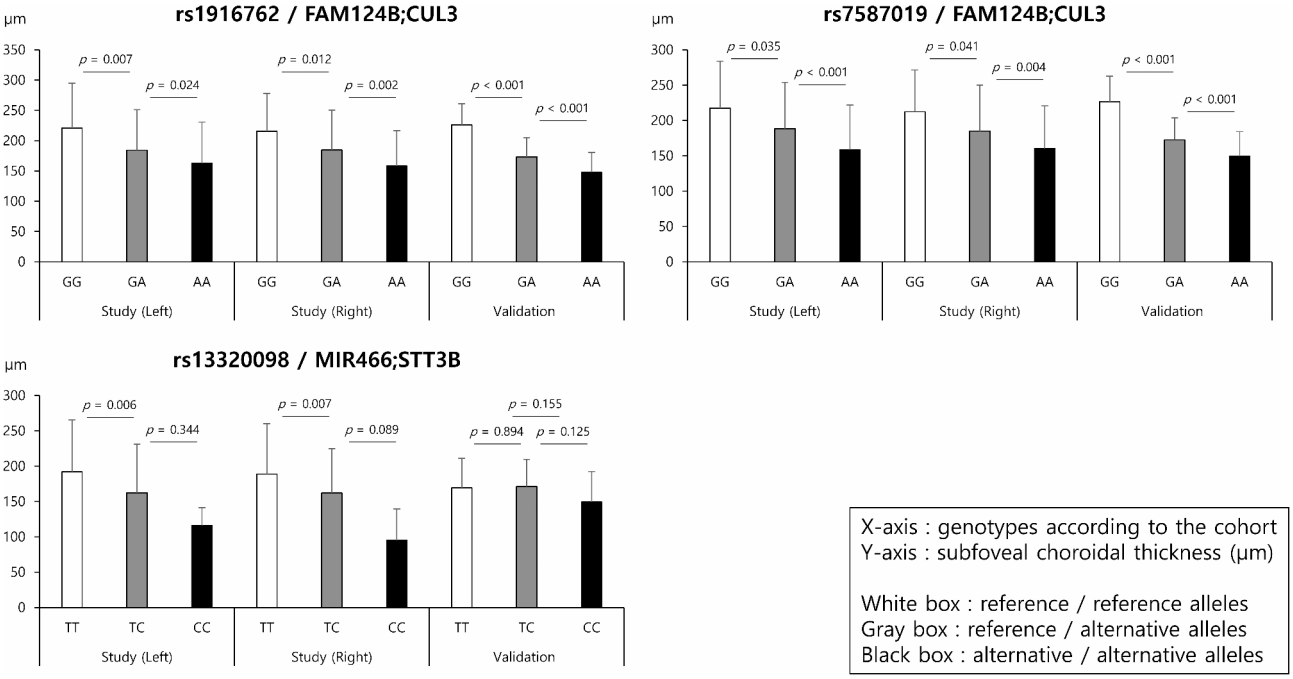

Fig. 3. Association between the subfoveal choroidal thickness and the genotypes of three SNPs, rs1916762 *FAM124B; CUL3*, rs7587019 *FAM124B; CUL3*, and rs13320098 *MIR466;STT3B*, in the discovery (study) dataset and the validation dataset.

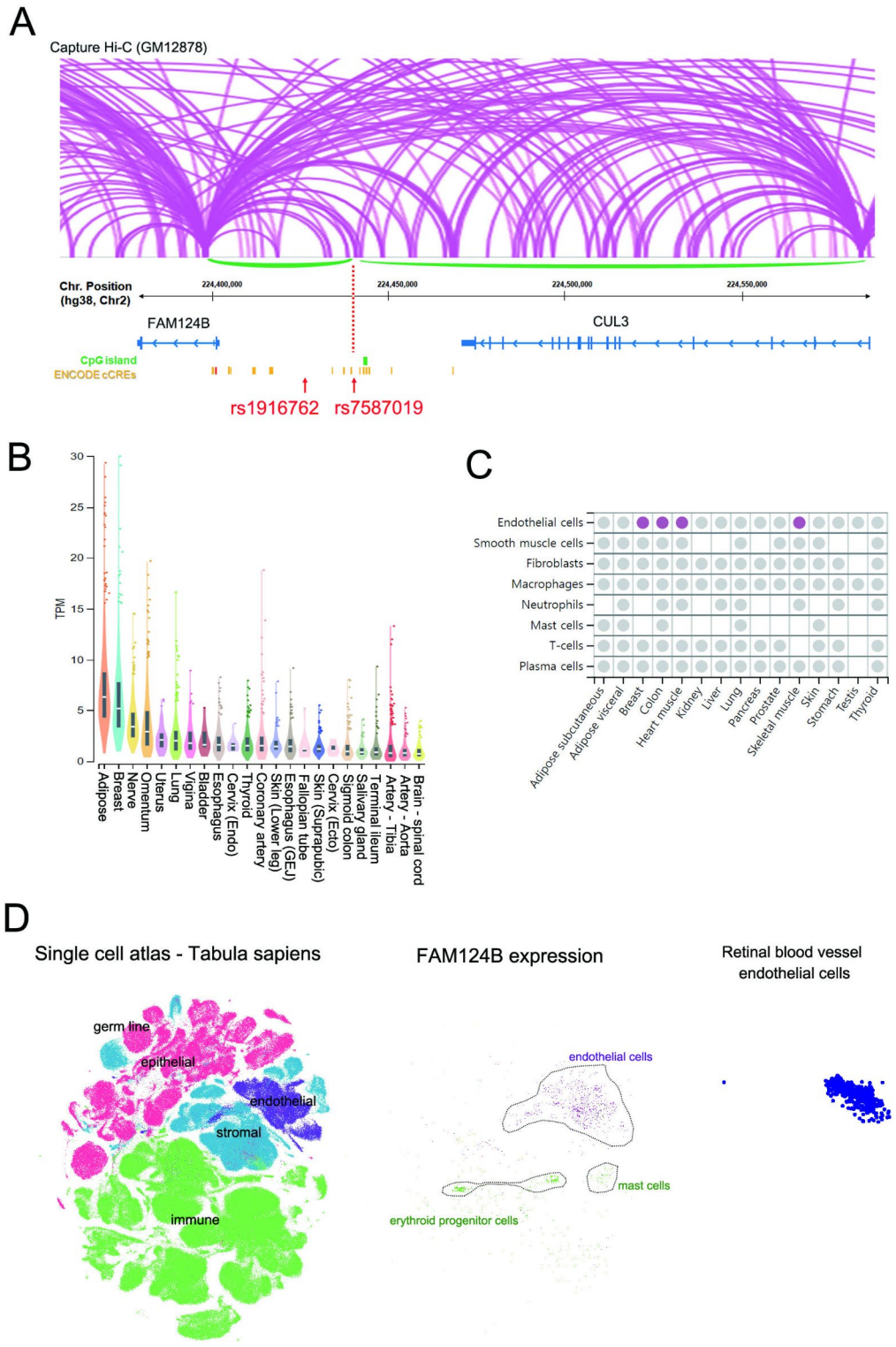

Fig. 4. Analyses of regulatory genes and target cells with rs1916762 and rs7587019 using the open database. (**A**) Schematic diagram depicting predicted interacting regions using the publicly available capture Hi-C visualization program (http://3dgenome.fsm.northwestern.edu/view.php) for two non-coding variants. (**B**) Data on high gene expression of *FAM124B* in top tissues. (**C**) Analysis of predominant cell types expressed in each tissue. Significant expression is indicated by the purple color. (**D**) Results of the single-cell expression analysis through Tabula Sapiens. The left panel depicts the distribution of cell types in a normal human, the middle panel shows cells sorted based on *FAM124B* expression, and the right panel highlights retinal vascular endothelial cells.

SNPs	Interacting gene	*P*-Value	NES	Tissue
rs1916762 (chr2_224426075_G_A)	***FAM124B***	2.1×10^{-9}	-0.31	Lung
	FAM124B	2.8×10^{-8}	-0.29	Thyroid
	AC073052.1	5.6×10^{-7}	0.36	Colon - Transverse
	AC073052.1	5.9×10^{-7}	0.25	Thyroid
	FAM124B	1.4×10^{-6}	-0.29	Esophagus - Mucosa
	FAM124B	4.4×10^{-6}	-0.17	Artery - Tibial
	AC073052.1	4.6×10^{-6}	0.25	Nerve - Tibial
	AC073052.1	2.7×10^{-5}	0.34	Spleen
	AC073052.1	3.8×10^{-5}	0.24	Muscle - Skeletal
	AC073052.1	3.8×10^{-5}	0.24	Adipose - Subcutaneous
	AC073052.1	7.1×10^{-5}	0.32	Cells - Cultured fibroblasts
	AC073052.1	1.1×10^{-4}	0.19	Esophagus - Mucosa
rs7587019 (chr2_224439834_G_A)	***FAM124B***	1.4×10^{-10}	-0.35	Lung
	AC073052.1	1.9×10^{-9}	0.31	Thyroid
	FAM124B	2.4×10^{-9}	-0.31	Thyroid
	AC073052.1	4.8×10^{-9}	0.45	Colon - Transverse
	AC073052.1	7.5×10^{-9}	0.36	Muscle - Skeletal
	FAM124B	5.2×10^{-8}	-0.52	Adrenal Gland
	AC073052.1	4.4×10^{-7}	0.3	Adipose - Subcutaneous
	AC073052.1	5.1×10^{-7}	0.35	Esophagus - Gastroesophageal Junction
	AC073052.1	9.0×10^{-7}	0.42	Spleen
	AC073052.1	1.4×10^{-6}	0.4	Cells - Cultured fibroblasts
	AC073052.1	1.6×10^{-6}	0.24	Esophagus - Mucosa
	FAM124B	1.6×10^{-6}	-0.32	Stomach
	FAM124B	3.6×10^{-6}	-0.17	Artery - Tibial
	FAM124B	3.9×10^{-6}	-0.32	Heart - Atrial Appendage
	AC073052.1	7.4×10^{-6}	0.21	Skin - Not Sun Exposed (Suprapubic)
	AC073052.1	1.0×10^{-5}	0.26	Skin - Sun Exposed (Lower leg)
	AC073052.1	1.4×10^{-5}	0.26	Nerve - Tibial
	AC073052.1	1.4×10^{-5}	0.32	Stomach
	AC073052.1	1.5×10^{-5}	0.19	Lung
	FAM124B	2.6×10^{-5}	-0.26	Esophagus - Mucosa
	AC073052.1	3.8×10^{-5}	0.33	Colon - Sigmoid
	FAM124B	3.9×10^{-5}	-0.28	Colon - Sigmoid
	AC073052.1	8.8×10^{-5}	0.26	Artery - Tibial
	AC073052.1	9.7×10^{-5}	0.16	Whole Blood

Table 3. Single-tissue eQTLs for rs1916762 and rs7587019. The data was aligned to the GRCh38/h38 reference genome. NES, normalized effect size, is defined as the slope of the linear regression, and is computed as the effect of the alternative allele (ALT) relative to the reference allele (REF) in the human genome reference. AC073052.1 (ENST00000622296.1, chr2:224467803–224474500) is predicted as a long non-coding RNA (pseudogene) in and near the *CUL3* gene.

and vascular and lymphatic endothelial cells. Single-cell RNA sequencing data from Tabula Sapiens revealed that *FAM124B* exhibited expression patterns in endothelial cells, erythroid progenitors, and mast cells, with a significant overlap observed in retinal vascular endothelial cells (Fig. 4D). Given the association of rs1916762 and rs7587019 with choroidal thickness, we propose that *FAM124B*, which is specifically expressed in vascular endothelial cells, is a target gene for the regulation of choroidal thickness. To investigate the molecular expression and function of *FAM124B* in vascular endothelial cells, we used HUVECs, which showed high expression of *FAM124B* in the Protein Atlas. The fluorescence of *FAM124B* was well-localized in the cytoplasm around the nucleus (Fig. 5A). Depletion of *FAM124B* using siRNAs significantly reduced the expression of the proliferation marker Ki67 (Fig. 5B, C), suggesting that *FAM124B* enhances the proliferation of vascular endothelial cells. However, no significant differences in cell migration were observed between the two groups (Fig. 5D, E).

Angiogenesis includes multiple steps such as proliferation and migration of vascular endothelial cells, and the maturation and remodeling of blood vessels, driven by various angiogenic factors like VEGF, FGF, and TGFs[24,25]. The Ras/MAPK pathway mainly regulates cell proliferation and gene expression, while the Rho GTPase pathway regulates cell migration by inducing the remodeling of the actin cytoskeleton and adhesion

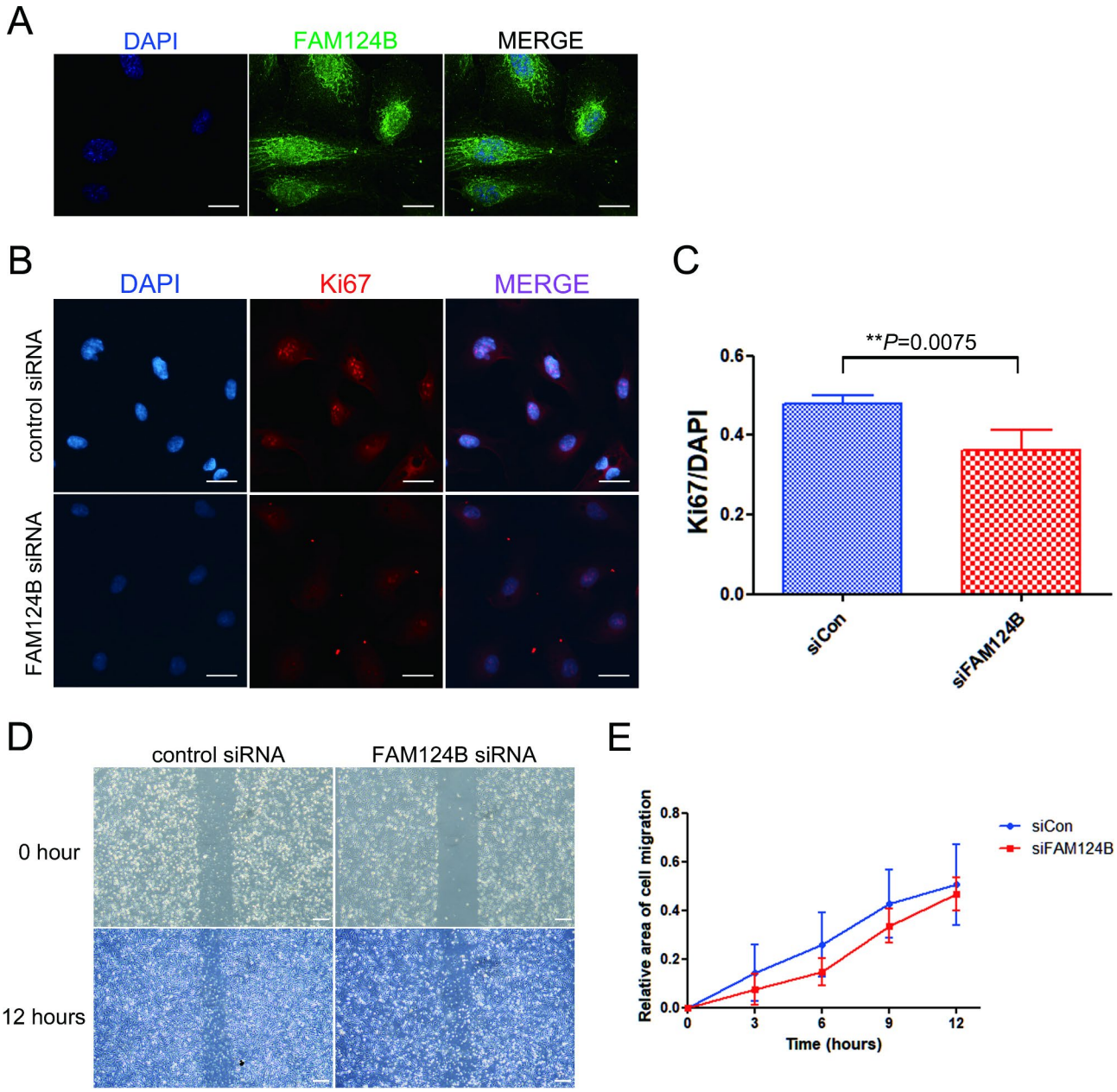

Fig. 5. Subcellular localization of *FAM124B* and proliferation and migration of *FAM124B*-depleted human umbilical vein endothelial cells (HUVECs). (**A**) Immunofluorescence staining of HUVECs using anti-*FAM124B* antibody (green). Scale bar size: 20 μm; 400x confocal microscopy (**B**) Expression pattern of the proliferation marker Ki67 in HUVECs after 48 h of treatment with control and *FAM124B* siRNAs. Scale bar size: 40 μm; 200x confocal microscopy (**C**) Relative proportion of Ki67-positive cells among DAPI-positive HUVECs after siRNA treatment. Each condition was measured in more than 600 cells in repeated experiments ($P=0.0075$, unpaired t-test). (**D**) Cell migration assay in HUVECs after treatment with control and *FAM124B* siRNAs. Scale bar size : 100 μm ; 40x light microscopy (**E**) Relative proportion of cell migration area over time (area without cells at each time point subtracted from the area without cells at 0 h, divided by the area without cells at 0 h) in four repeated experiment.

complexes[24,26]. In our study, the increase in HUVEC proliferation by FAM124B is hypothesized to be due to its exclusive effect on cellular proliferation, without involvement in the mechanisms regulating the actin cytoskeleton or adhesion complexes through the Rho GTPase pathway and integrin signaling.

Discussion

We conducted GWAS to discover susceptibility genes associated with the subfoveal choroidal thickness in the population-based KLoSHA/KLOSCAD cohort, followed by validation in the Bundang AMD cohort. We

revealed that the SNPs rs1916762 and rs7587019 between the *FAM124B* and *CUL3* genes (intergenic) affected SFCT, and the SFCT was significantly related to the genotypes.

Genetic analysis of pachychoroid spectrum diseases presenting with thickened choroid and choroidal vascular hyperpermeability has been conducted[27]. GWAS investigations have reported *ARMS2/HTRA1*, *CFH*, *COL4A3*, and *B3GALTL* as strong susceptibility genes for PCV and CSC[16,17,19]. Choroid thinning is recognized as a key factor in the development of AMD. Our goal was to identify the genes associated with choroid thinning in the elderly to discover the genetic causes of AMD. Hence, it would be preferable to indicate that the AMD patient group was chosen as the validation set.

FAM124B is a protein-coding gene, and only a few studies have explored its role in human diseases. Li et al. demonstrated that *FAM124B* has a higher DNA methylation level in ER+/PR+breast cancer compared with ER-/PR- breast cancers[28]. One GWAS revealed that the SNP rs1523921 (intergenic between *CUL3* and *FAM124B)* is associated with anorexia nervosa[29]. Another study reported that in patients with acute myeloid leukemia, *FAM124B* is associated with acute myeloid leukemia (AML) prognosis[30]. At the molecular level, *FAM124B* was identified as a potential interacting partner of CHD7 and CHD8 (chromodomain helicase DNA binding domain) containing complex, and thus related to the pathogenesis of CHARGE syndrome and neurodevelopmental disorders[31].

To the best of our knowledge, the *FAM124B* gene has not been directly associated with ocular diseases. In our study, we observed a potential association between the *FAM124B* gene and choroidal structure. To further investigate this hypothesis, we conducted an experiment using HUVEC. The results revealed that inhibition of *FAM124B* significantly reduced the expression of the proliferation marker Ki67, indicating the potential role of the *FAM124B* gene in enhancing the proliferation of vascular endothelial cells in the choroid. Overall, it appears plausible that individuals with alternative/alternative alleles (AA) in *CUL3* and *FAM124B* exhibit thinner subfoveal choroidal thickness than those with reference/reference alleles (GG), considering that the two SNPs (rs1916762 and rs7587019) function as *FAM124B* cis-regulatory elements both in silico and experimentally.

CUL3 (E3 ubiquitin ligase Cullin 3) regulates cellular protein composition by providing target recognition and specificity to the ubiquitin-dependent proteasomal degradation pathway[32]. Moreover, *CUL3* mutations cause familial hyperkalemic hypertension by affecting vascular tone and renal sodium transport[33]. *CUL3* ubiquitin ligase maintains normal cardiovascular and renal physiology, and thus regulates blood pressure[34]. Furthermore, patients with diabetes and *CUL3 dysfunction* exhibit vasoconstriction by increased abundance of WNK3, RhoA/ROCK activity, and phosphodiesterase 5, thereby enhancing sodium reabsorption, leading to increased risk of diabetic nephropathy[35].

In clinical settings, previous studies have yielded conflicting findings regarding the association between choroidal thickness and systemic vascular diseases. Xu et al. highlighted that patients with diabetes mellitus presented with a slightly significant thickening of the subfoveal choroid, while those diagnosed with diabetic retinopathy were not characterized by choroidal thickness abnormalities[36]. Meanwhile, other studies showed reduction in the SFCT in patients with diabetes or diabetic retinopathy[37–39]. The Montrachet population-based study suggested that the SFCT is not an appropriate biomarker for cardiovascular diseases[40]. In our study, we propose that the vascular proliferation of *FAM124B*, known to affect systemic vascular diseases, is likely to affect choroidal thickness. Moreover, choroidal thickness in neovascular AMD or geographical atrophy is known to be significantly reduced compared to normal individuals[41–43]. Therefore, our study results are potentially useful for clinicians and researchers in targeting choroidal vascular proliferation as a mechanism of AMD treatment.

This study had certain limitations. We focused on SNPs with p-values $< 1.0 \times 10^{-4}$ identified in the GWAS, a threshold that is typically not accepted as a level of significance in standard GWAS investigations. By relaxing the threshold to 1.0×10^{-4} for each eye, we aim to identify a broader range of potentially relevant SNPs. Crucially, our method mandates that SNPs meet this threshold in both eyes, providing a safeguard against false positives that might occur by chance in only one eye. This bilateral consistency requirement improves the reliability of our findings. We believe that SNPs consistently associated across both eyes are more likely to be genuine genetic factors influencing choroidal thickness, thereby enhancing the biological significance of our results. We recognize that this approach may increase the likelihood of false positives compared to the conventional threshold. Thus, we stress the need for further validation and functional studies to confirm the biological relevance of the identified SNPs.Additionally, the discovery cohort consisted solely of individuals without retinal disease, whereas the validation cohort comprised patients with AMD. This distinction indicates that a direct comparison of the SFCTs between the discovery and validation datasets may not be perfectly aligned. Moreover, our investigation included an *in vitro* HUVEC experiment targeting the *FAM124B* gene, conducting siRNA transfection with the proliferation marker Ki67. The rationale for conducting the experiment with *FAM124B* siRNA transfection rather than *CUL3* is as follows: (1) the intergenic location of the discovered single nucleotide variants (SNVs) is closer to *FAM124B*, suggesting a higher relevance, (2) in existing databases, *CUL3* is associated with immune cells and shows high expression across all tissue types, while *FAM124B* displays a vascular-specific expression pattern. Additional proliferation markers, such as CD34 and, if necessary, *CUL3* siRNA transfection, could be employed for further *in vitro* studies to elucidate the role of both genes in choroidal thickness.

In conclusion, the *FAM124B* gene has been identified as a potential contributor to subfoveal choroidal thickness. The genotypes of the identified SNPs may be linked to variations in subfoveal choroidal thickness. Further studies are warranted to investigate the effect of genetic factors on choroidal thickness.

Data availability

Data availability statement (mandatory) : Raw data, functional analysis sources and descriptions will be provided upon request. Correspondence should be addressed to Se Joon Woo. (Tel: +82-31-787-7377, Fax: +82-31-787-4057, E-mail: sejoon1@snu.ac.kr)

Received: 20 March 2024; Accepted: 13 September 2024
Published online: 09 October 2024

References

1. Ferrara, D. et al. En face enhanced-depth swept-source optical coherence tomography features of chronic central serous chorioretinopathy. *Ophthalmology* **121**, 719–726. https://doi.org/10.1016/j.ophtha.2013.10.014 (2014).
2. Pang, C. E. & Freund, K. B. Pachychoroid neovasculopathy. *Retina* **35**, 1–9. https://doi.org/10.1097/IAE.0000000000000331 (2015).
3. Pauleikhoff, D., Chen, J. C., Chisholm, I. H. & Bird, A. C. Choroidal perfusion abnormality with age-related Bruch's membrane change. *Am. J. Ophthalmol.* **109**, 211–217. https://doi.org/10.1016/s0002-9394(14)75989-6 (1990).
4. Warrow, D. J., Hoang, Q. V. & Freund, K. B. Pachychoroid pigment epitheliopathy. *Retina* **33**, 1659–1672. https://doi.org/10.1097/IAE.0b013e3182953df4 (2013).
5. Margolis, R. & Spaide, R. F. A pilot study of enhanced depth imaging optical coherence tomography of the choroid in normal eyes. *Am. J. Ophthalmol.* **147**, 811–815. https://doi.org/10.1016/j.ajo.2008.12.008 (2009).
6. Spaide, R. F., Koizumi, H. & Pozzoni, M. C. Enhanced depth imaging spectral-domain optical coherence tomography. *Am. J. Ophthalmol.* **146**, 496–500. https://doi.org/10.1016/j.ajo.2008.05.032 (2008).
7. Chung, S. E., Kang, S. W., Lee, J. H. & Kim, Y. T. Choroidal thickness in polypoidal choroidal vasculopathy and exudative age-related macular degeneration. *Ophthalmology* **118**, 840–845. https://doi.org/10.1016/j.ophtha.2010.09.012 (2011).
8. Dansingani, K. K., Balaratnasingam, C., Naysan, J. & Freund, K. B. En face imaging of pachychoroid spectrum disorders with swept-source optical coherence tomography. *Retina* **36**, 499–516. https://doi.org/10.1097/IAE.0000000000000742 (2016).
9. Edwards, A. O. et al. Complement factor H polymorphism and age-related macular degeneration. *Science* **308**, 421–424. https://doi.org/10.1126/science.1110189 (2005).
10. Haines, J. L. et al. Complement factor H variant increases the risk of age-related macular degeneration. *Science* **308**, 419–421. https://doi.org/10.1126/science.1110359 (2005).
11. Klein, R. J. et al. Complement factor H polymorphism in age-related macular degeneration. *Science* **308**, 385–389. https://doi.org/10.1126/science.1109557 (2005).
12. Arakawa, S. et al. Genome-wide association study identifies two susceptibility loci for exudative age-related macular degeneration in the Japanese population. *Nat. Genet.* **43**, 1001–1004. https://doi.org/10.1038/ng.938 (2011).
13. Chen, L. J. Genetic association of age-related macular degeneration and polypoidal choroidal vasculopathy. *Asia Pac. J. Ophthalmol. (Phila)* **9**, 104–109. https://doi.org/10.1097/01.APO.0000656976.47696.7d (2020).
14. Chen, W. et al. Genetic variants near TIMP3 and high-density lipoprotein-associated loci influence susceptibility to age-related macular degeneration. *Proc. Natl. Acad. Sci. U S A* **107**, 7401–7406. https://doi.org/10.1073/pnas.0912702107 (2010).
15. Dewan, A. et al. HTRA1 promoter polymorphism in wet age-related macular degeneration. *Science* **314**, 989–992. https://doi.org/10.1126/science.1133807 (2006).
16. Hosoda, Y. et al. CFH and VIPR2 as susceptibility loci in choroidal thickness and pachychoroid disease central serous chorioretinopathy. *Proc. Natl. Acad. Sci. U S A* **115**, 6261–6266. https://doi.org/10.1073/pnas.1802212115 (2018).
17. Mori, Y. et al. Genome-wide survival analysis for macular neovascularization development in central serous chorioretinopathy revealed shared genetic susceptibility with polypoidal choroidal vasculopathy. *Ophthalmology* **129**, 1034–1042. https://doi.org/10.1016/j.ophtha.2022.04.018 (2022).
18. Neale, B. M. et al. Genome-wide association study of advanced age-related macular degeneration identifies a role of the hepatic lipase gene (LIPC). *Proc. Natl. Acad. Sci. U S A* **107**, 7395–7400. https://doi.org/10.1073/pnas.0912019107 (2010).
19. Thee, E. F. et al. The phenotypic course of age-related macular degeneration for ARMS2/HTRA1: The EYE-RISK Consortium. *Ophthalmology* **129**, 752–764. https://doi.org/10.1016/j.ophtha.2022.02.026 (2022).
20. Ryoo, N. K. et al. Thickness of retina and choroid in the elderly population and its association with complement factor H polymorphism: KLoSHA Eye study. *PLoS ONE* **13**, e0209276. https://doi.org/10.1371/journal.pone.0209276 (2018).
21. Han, J. W. et al. Overview of the Korean longitudinal study on cognitive aging and dementia. *Psychiatry Investig.* **15**, 767–774. https://doi.org/10.30773/pi.2018.06.02 (2018).
22. Kim, H. M. et al. Association between retinal layer thickness and cognitive decline in older adults. *JAMA Ophthalmol.* **140**, 683–690. https://doi.org/10.1001/jamaophthalmol.2022.1563 (2022).
23. Joo, K., Mun, Y. S., Park, S. J., Park, K. H. & Woo, S. J. Ten-year progression from intermediate to exudative age-related macular degeneration and risk factors: Bundang AMD Cohort Study Report 1. *Am. J. Ophthalmol.* **224**, 228–237. https://doi.org/10.1016/j.ajo.2020.11.012 (2021).
24. Liu, Z. L., Chen, H. H., Zheng, L. L., Sun, L. P. & Shi, L. Angiogenic signaling pathways and anti-angiogenic therapy for cancer. *Signal. Transduct. Target. Ther.* **8**, 198. https://doi.org/10.1038/s41392-023-01460-1 (2023).
25. Wang, S. et al. Control of endothelial cell proliferation and migration by VEGF signaling to histone deacetylase 7. *Proc. Natl. Acad. Sci. U S A* **105**, 7738–7743. https://doi.org/10.1073/pnas.0802857105 (2008).
26. Devreotes, P. & Horwitz, A. R. Signaling networks that regulate cell migration. *Cold Spring Harb. Perspect. Biol.* **7**, a005959. https://doi.org/10.1101/cshperspect.a005959 (2015).
27. Miyake, M. et al. Choroidal neovascularization in eyes with choroidal vascular hyperpermeability. *Invest. Ophthalmol. Vis. Sci.* **55**, 3223–3230. https://doi.org/10.1167/iovs.14-14059 (2014).
28. Li, L. et al. Estrogen and progesterone receptor status affect genome-wide DNA methylation profile in breast cancer. *Hum. Mol. Genet.* **19**, 4273–4277. https://doi.org/10.1093/hmg/ddq351 (2010).
29. Boraska, V. et al. A genome-wide association study of anorexia nervosa. *Mol. Psychiatry* **19**, 1085–1094. https://doi.org/10.1038/mp.2013.187 (2014).
30. Kuang, Y., Wang, Y., Cao, X., Peng, C. & Gao, H. New prognostic factors and scoring system for patients with acute myeloid leukemia. *Oncol. Lett.* **22**, 823. https://doi.org/10.3892/ol.2021.13084 (2021).
31. Batsukh, T. et al. Identification and characterization of FAM124B as a novel component of a CHD7 and CHD8 containing complex. *PLoS ONE* **7**, e52640. https://doi.org/10.1371/journal.pone.0052640 (2012).
32. De Rubeis, S. et al. Synaptic, transcriptional and chromatin genes disrupted in autism. *Nature* **515**, 209–215. https://doi.org/10.1038/nature13772 (2014).
33. Morandell, J. et al. Cul3 regulates cytoskeleton protein homeostasis and cell migration during a critical window of brain development. *Nat. Commun.* **12**, 3058. https://doi.org/10.1038/s41467-021-23123-x (2021).
34. Schumacher, F. R. et al. Characterisation of the Cullin-3 mutation that causes a severe form of familial hypertension and hyperkalaemia. *EMBO Mol. Med.* **7**, 1285–1306. https://doi.org/10.15252/emmm.201505444 (2015).
35. Abdel Khalek, W. et al. Severe arterial hypertension from Cullin 3 mutations is caused by both renal and vascular effects. *J. Am. Soc. Nephrol.* **30**, 811–823. https://doi.org/10.1681/ASN.2017121307 (2019).
36. Xu, J. et al. Subfoveal choroidal thickness in diabetes and diabetic retinopathy. *Ophthalmology* **120**, 2023–2028. https://doi.org/10.1016/j.ophtha.2013.03.009 (2013).
37. Querques, G. et al. Enhanced depth imaging optical coherence tomography in type 2 diabetes. *Invest. Ophthalmol. Vis. Sci.* **53**, 6017–6024. https://doi.org/10.1167/iovs.12-9692 (2012).

38. Regatieri, C. V., Branchini, L., Carmody, J., Fujimoto, J. G. & Duker, J. S. Choroidal thickness in patients with diabetic retinopathy analyzed by spectral-domain optical coherence tomography. *Retina* **32**, 563–568. https://doi.org/10.1097/IAE.0b013e31822f5678 (2012).
39. Vujosevic, S., Martini, F., Cavarzeran, F., Pilotto, E. & Midena, E. Macular and peripapillary choroidal thickness in diabetic patients. *Retina* **32**, 1781–1790. https://doi.org/10.1097/IAE.0b013e31825db73d (2012).
40. Arnould, L. et al. Subfoveal choroidal thickness, cardiovascular history, and risk factors in the elderly: The Montrachet study. *Invest. Ophthalmol. Vis. Sci.* **60**, 2431–2437. https://doi.org/10.1167/iovs.18-26488 (2019).
41. Kim, J. H., Kim, J. R., Kang, S. W., Kim, S. J. & Ha, H. S. Thinner choroid and greater drusen extent in retinal angiomatous proliferation than in typical exudative age-related macular degeneration. *Am. J. Ophthalmol.* **155**, 743–749. https://doi.org/10.1016/j.ajo.2012.11.001 (2013).
42. Manjunath, V., Goren, J., Fujimoto, J. G. & Duker, J. S. Analysis of choroidal thickness in age-related macular degeneration using spectral-domain optical coherence tomography. *Am. J. Ophthalmol.* **152**, 663–668. https://doi.org/10.1016/j.ajo.2011.03.008 (2011).
43. Yamazaki, T., Koizumi, H., Yamagishi, T. & Kinoshita, S. Subfoveal choroidal thickness after ranibizumab therapy for neovascular age-related macular degeneration: 12-month results. *Ophthalmology* **119**, 1621–1627. https://doi.org/10.1016/j.ophtha.2012.02.022 (2012).

Author contributions

H.M.K and K.J. : conception and design, collection and/or assembly of data, data analysis and interpretation, manuscript writing, final approval of manuscript. M.K, Y.J.P, J.W.H., K.W.K., and S.L. : collection and/or assembly of data, data analysis and interpretation, S.J.W. : conception and design, financial support, administrative support, manuscript writing, final approval of manuscript.

Funding

This research was supported by the National Research Foundation (NRF) funded by the Korean government (Ministry of Science and ICT) (No. 2022R1A2C4002114, RS-2023-00248480), a research grant from Seoul National University Bundang Hospital (09-2022-0002, 13-2024-0001) and a grant from the Korean Health Technology R&D Project, Ministry of Health and Welfare, Republic of Korea [grant No. HI09C1379 (A092077)]. The funding organizations played no role in the design or conduct of this study.

Declarations

Competing interests

The authors declare no competing interests.

Ethics approval

I attest that the research included in this report was conducted in a manner consistent with the principles of research ethics, including those described in the Declaration of Helsinki and the Belmont Report. This research was conducted with the voluntary informed consent of all research participants, free of coercion or coercive circumstances, and received Institutional Review Board (IRB) approval consistent with the principles of research ethics and the legal requirements of the lead authors' jurisdiction(s).

Additional information

Correspondence and requests for materials should be addressed to S.J.W.

Terms and Conditions

Springer Nature journal content, brought to you courtesy of Springer Nature Customer Service Center GmbH (“Springer Nature”).
Springer Nature supports a reasonable amount of sharing of research papers by authors, subscribers and authorised users (“Users”), for small-scale personal, non-commercial use provided that all copyright, trade and service marks and other proprietary notices are maintained. By accessing, sharing, receiving or otherwise using the Springer Nature journal content you agree to these terms of use (“Terms”). For these purposes, Springer Nature considers academic use (by researchers and students) to be non-commercial.
These Terms are supplementary and will apply in addition to any applicable website terms and conditions, a relevant site licence or a personal subscription. These Terms will prevail over any conflict or ambiguity with regards to the relevant terms, a site licence or a personal subscription (to the extent of the conflict or ambiguity only). For Creative Commons-licensed articles, the terms of the Creative Commons license used will apply.
We collect and use personal data to provide access to the Springer Nature journal content. We may also use these personal data internally within ResearchGate and Springer Nature and as agreed share it, in an anonymised way, for purposes of tracking, analysis and reporting. We will not otherwise disclose your personal data outside the ResearchGate or the Springer Nature group of companies unless we have your permission as detailed in the Privacy Policy.
While Users may use the Springer Nature journal content for small scale, personal non-commercial use, it is important to note that Users may not:

1. use such content for the purpose of providing other users with access on a regular or large scale basis or as a means to circumvent access control;
2. use such content where to do so would be considered a criminal or statutory offence in any jurisdiction, or gives rise to civil liability, or is otherwise unlawful;
3. falsely or misleadingly imply or suggest endorsement, approval , sponsorship, or association unless explicitly agreed to by Springer Nature in writing;
4. use bots or other automated methods to access the content or redirect messages
5. override any security feature or exclusionary protocol; or
6. share the content in order to create substitute for Springer Nature products or services or a systematic database of Springer Nature journal content.

In line with the restriction against commercial use, Springer Nature does not permit the creation of a product or service that creates revenue, royalties, rent or income from our content or its inclusion as part of a paid for service or for other commercial gain. Springer Nature journal content cannot be used for inter-library loans and librarians may not upload Springer Nature journal content on a large scale into their, or any other, institutional repository.
These terms of use are reviewed regularly and may be amended at any time. Springer Nature is not obligated to publish any information or content on this website and may remove it or features or functionality at our sole discretion, at any time with or without notice. Springer Nature may revoke this licence to you at any time and remove access to any copies of the Springer Nature journal content which have been saved.
To the fullest extent permitted by law, Springer Nature makes no warranties, representations or guarantees to Users, either express or implied with respect to the Springer nature journal content and all parties disclaim and waive any implied warranties or warranties imposed by law, including merchantability or fitness for any particular purpose.
Please note that these rights do not automatically extend to content, data or other material published by Springer Nature that may be licensed from third parties.
If you would like to use or distribute our Springer Nature journal content to a wider audience or on a regular basis or in any other manner not expressly permitted by these Terms, please contact Springer Nature at

onlineservice@springernature.com